The interaction of mammalian mitochondrial translational initiation factor 3 with ribosomes: evolution of terminal extensions in IF3$_{mt}$

Md. Emdadul Haque, Domenick Grasso and Linda L. Spremulli*

Department of Chemistry, University of North Carolina at Chapel Hill, Chapel Hill, NC-27599-3290, USA

ABSTRACT

Mammalian mitochondrial initiation factor 3 (IF3$_{mt}$) has a central region with homology to bacterial IF3. This homology region is preceded by an N-terminal extension and followed by a C-terminal extension. The role of these extensions on the binding of IF3$_{mt}$ to mitochondrial small ribosomal subunits (28S) was studied using derivatives in which the extensions had been deleted. The K_d for the binding of IF3$_{mt}$ to 28S subunits is ~30 nM. Removal of either the N- or C-terminal extension has almost no effect on this value. IF3$_{mt}$ has very weak interactions with the large subunit of the mitochondrial ribosome (39S) ($K_d = 1.5 \mu M$). However, deletion of the extensions results in derivatives with significant affinity for 39S subunits ($K_d = 0.12–0.25 \mu M$). IF3$_{mt}$ does not bind 55S monosomes, while the deletion derivative binds slightly to these particles. IF3$_{mt}$ is very effective in dissociating 55S ribosomes. Removal of the N-terminal extension has little effect on this activity. However, removal of the C-terminal extension leads to a complex dissociation pattern due to the high affinity of this derivative for 39S subunits. These data suggest that the extensions have evolved to ensure the proper dissociation of IF3$_{mt}$ from the 28S subunits upon 39S subunit joining.

INTRODUCTION

The protein synthesizing machinery of mammalian mitochondria has several distinct differences from the prokaryotic and eukaryotic cytoplasmic systems. The mammalian mitochondrial genome consists of only 16 000 bp that encode 13 polypeptides, 2 rRNAs and 22 tRNAs. These 13 polypeptides are essential for oxidative phosphorylation. Mitochondrial ribosomes are 55S particles with 28S small and 39S large subunits (1). Mammalian mitochondrial ribosomes are protein rich and have a number of distinguishing features as revealed by cryo-electron microscopy (2). Very limited information has been reported on the mechanism of translational initiation in this organelle. Only two initiation factors have been identified to date, initiation factor 2 (IF2$_{mt}$) promotes the binding of fMet-tRNA to the ribosome, while mitochondrial initiation factor 3 (IF3$_{mt}$) facilitates the dissociation of the mitochondrial 55S ribosome into subunits (3–11).

In bacteria, IF3 plays a vital role in translational initiation. This highly basic protein promotes the dissociation of 70S ribosomes into 30S and 50S subunits. This factor also enhances codon–anticodon interactions at the P-site, promotes the shift in position of the mRNA on the 30S subunit from the standby to a decoding position and increases the rate of dissociation of non-canonical 30S initiation complexes (12–20). IF3 maximizes the advantage of the initiator tRNA for binding to 30S subunits and for subunit joining (21).

A considerable amount of information is available on the binding of *Escherichia coli* IF3 to 30S subunits, and several views of its location on the ribosome have been reported (13,17,18,22–25). A number of biochemical and biophysical studies suggest that *E. coli* IF3 interacts with 30S subunits in the region of the platform, cleft and the head, facing the 50S subunit (13,18,25–27). A range of equilibrium dissociation constants (from 30 to 100 nM) have been reported for the binding of IF3 to 30S subunits The association rate constants reported (10^4 to $10^8 M^{-1} s^{-1}$) and the reported dissociation rate constants (0.44 to 20 s^{-1}) vary considerably (28–30).

Escherichia coli IF3 consists of two domains (N- and C-terminal) that are joined by a flexible linker (Figure 1) (31). The C-terminal domain of *E. coli* IF3 is thought to perform most of the functions of this factor while the N-terminal domain stabilizes the binding of IF3 to the 30S subunit (17). Recent studies indicate that the N-terminal domain modulates the association and dissociation of IF3 from the 30S subunit through a fluctuating interaction with the neck region of the 30S subunit (19).

*To whom correspondence should be addressed. Tel: +1 919 966 1567; Fax: +1 919 843 1580; Email: linda_spremulli@unc.edu
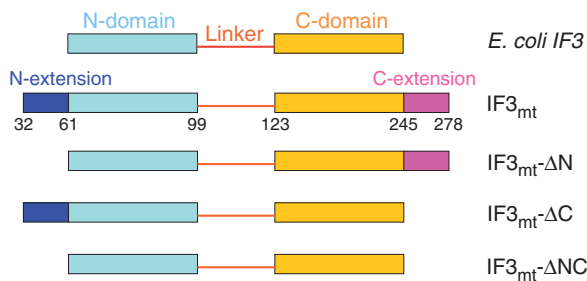
Figure 1. Comparison of the domain structure of *E. coli* IF3 to that of human IF3$_{mt}$ and its deletion derivatives. IF3$_{mt}$ is shown without the import signal which was removed in the preparation of the full-length factor. The three deletion derivatives used here are shown schematically and were prepared as described previously (10). The numbers represent the amino acid residue at the beginning of the indicated domain. The numbering for IF3$_{mt}$ is based on the complete protein-coding region including the mitochondrial import sequence.

The IF3$_{mt}$ has a central region with homology to the bacterial factor that is surrounded by N-terminal and C-terminal extensions (Figure 1). The crystal structure of IF3$_{mt}$ is not known, but the N-domain has been modeled to have a structure similar to that of the bacterial factor (11). The C-domain of human IF3$_{mt}$ cannot be modeled on the structure of the bacterial factor due to the low degree of homology. However, the structure of the C-domain (without the C-terminal extension) of mouse IF3$_{mt}$ has been determined using NMR (PDB coordinates 2CRQ, to be published). This region of the mitochondrial factor has a similar overall structure to that of the C-domain of *E. coli* IF3 although IF3$_{mt}$ has an additional β-sheet and a small extra helical turn. The structures of the linker region and of the N-terminal and C-terminal extensions remain unknown. The mature form of IF3$_{mt}$ and derivatives in which the extensions have been deleted are active in initiation complex formation on both mitochondrial 55S ribosomes and on bacterial 70S ribosomes (10,11) but the C-terminal extension appears to play a role in the dissociation of fMet-tRNA bound to 28S subunits in the absence of mRNA (10). In the present study, we have investigated the interactions of IF3$_{mt}$, and derivatives of this factor lacking the extensions, with mitochondrial 28S and 39S subunits and with 55S ribosomes. Our results suggest that the extensions help to ensure the proper dissociation of IF3$_{mt}$ from the 28S subunits upon 39S joining.

MATERIALS AND METHODS

Materials

Regular chemicals were purchased from Sigma-Aldrich or Fisher Scientific. A rabbit polyclonal primary antibody to the region of IF3$_{mt}$ homologous to the bacterial factors was made by Pacific Immunology Corporation. Goat antirabbit IgG antibody coupled to alkaline phosphatase was purchased from Sigma and used as a secondary antibody. Protein-free blocking agent was purchased from Pierce Technologies. Microcon-100 spin columns and pure nitrocellulose membrane filters were purchased from Millipore Corporation. The Bio-Dot Microfiltration

apparatus was from Bio-Rad. Research-grade CM5 sensor chips, 1-ethyl-3-(3-dimethylaminopropyl)-carbodiimide (EDC), *N*-hydroxysuccinimide (NHS) and 2-(2-pyridinyldithio)-ethaneamine hydrochloride (PDEA, thio-coupling reagent) were obtained from Biacore Company. Bovine mitochondrial ribosomes (55S), ribosomal subunits (28S and 39S), bovine IF2$_{mt}$ and yeast [^{35}S]fMet-tRNA were prepared as described (2,8,32,33).

Cloning, expression and purification

Deletion derivatives of IF3$_{mt}$ were purified as described previously (10). The three deletion derivatives of IF3$_{mt}$ (Figure 1): IF3$_{mt}$−ΔN (N-terminal extension deleted), IF3$_{mt}$−ΔC (C-terminal extension deleted) and IF3$_{mt}$−ΔNC (both N- and C-terminal extensions deleted) did not require further purification following the Ni-NTA column. Full-length IF3$_{mt}$ was purified on S-Sepharose as described (34).

Quantitation of the binding of IF3$_{mt}$ and its derivatives to mitochondrial 28S subunits using Microcon centrifugation

Ribosome-binding reactions (100 µl) were carried out in Binding Buffer (10 mM Tris–HCl, pH 7.6, 40 mM KCl, 7.5 mM MgCl$_2$, 1 mM dithiothreitol [DTT] and 0.1 mM spermine), 50 nM 28S subunits (5 pmol) and 2.5 to 30 nM IF3$_{mt}$ or its derivatives. The samples were incubated for 20 min at 25°C. The reaction mixtures were added to the Microcon spin columns and centrifuged for 2 min at 12 000 r.p.m. (10 900*g*). The Microcon columns were washed with 100 µl Binding Buffer and centrifuged as above. The IF3$_{mt}$ retained on the filter with 28S subunits was recovered by inverting the column, adding 100 µl Binding Buffer and centrifuging for 1 min as described above. The sample containing the bound IF3$_{mt}$ was applied to the dot blot apparatus and the binding of IF3$_{mt}$ to 28S subunits was quantified colorimetrically as described below. The amount of bound protein was determined from a calibration curve obtained using 28S subunits (5 pmol) and varying amounts of IF3$_{mt}$ (0.25–0.75 pmol). The calibration curve was linear over this range (Supplementary Data, Figure S1A).

To estimate the apparent equilibrium dissociation constant for the interaction of IF3$_{mt}$ and its derivatives with 28S subunits, it was necessary to determine the percentage of active molecules. These values were determined as described previously (6) and indicated that the IF3$_{mt}$ was almost 100% active while the 28S subunits were 25–50% active.

Binding of IF3$_{mt}$ to 28S, 39S and 55S ribosomes using sucrose density gradient centrifugation

Samples (100 µl) were prepared in Binding Buffer containing IF3$_{mt}$ alone, ribosomes alone or ribosomes and IF3$_{mt}$ together. Following incubation for 20 min at 25°C, the samples were applied to a cold 4.8 ml 10–30% sucrose density gradient prepared in Binding Buffer. The concentration of 28S subunits used was 70 nM and the IF3$_{mt}$ concentration was varied from 2.5 to 100 nM. The gradients were centrifuged for 1 h 45 min at 48 000 r.p.m.

in a Beckman SW55 Ti rotor. Sucrose gradients were fractionated on an ISCO gradient fractionator at a flow rate of 0.8 ml/min and fractions (~200 µl) were collected. The material in appropriate fractions was applied to the dot blot apparatus and analysed as described subsequently. Two control experiments were performed: $IF3_{mt}$ alone and ribosomes or ribosomal subunits alone. The material in these control fractions was also analysed using the dot blot for the determination of background intensity and this background was subtracted from the intensity obtained when ribosomes were incubated with $IF3_{mt}$. The presence of sucrose in the gradient fractions increased the background in the dot blot considerably. A comparison of the dot blot signal from the samples-containing ribosomes and $IF3_{mt}$ together to the signal from the controls allowed an estimation of the amount of $IF3_{mt}$ bound to ribosomes or ribosomal subunits.

Quantitative immunological detection for $IF3_{mt}$

Dot blots were performed basically as described previously (6). Image quantification of the intensities of the blots was carried out using the UN-SCAN IT Gel software.

Dissociation of mitochondrial 55S ribosomes by $IF3_{mt}$ and its extension truncated derivatives

Mitochondrial ribosomes (56 nM) were incubated in the presence or absence of $IF3_{mt}$ or its truncated derivatives (350 nM, 35 pmol) in 100 µl of Gradient Buffer (25 mM Tris–HCl, pH 7.6, 5 mM $MgCl_2$, 40 mM KCl and 1 mM DTT) for 15 min at 37°C. After incubation, reaction mixtures were placed on ice for 10 min and then layered onto a cold 4.8 ml 10–30% linear sucrose gradient prepared in the Gradient Buffer. Gradients were centrifuged for 1 h and 45 min in SW55 Ti rotor and fractionated using an ISCO gradient fractionator while monitoring the absorbance at 254 nm using an ISCO UA-5 monitor.

Initiation complex formation on mitochondrial ribosomes

Stimulation of initiation complex formation by $IF3_{mt}$ was examined by measuring the increase of [^{35}S]fMet-tRNA binding to 55S ribosomes in a filter-binding assay (11). Reaction mixtures (100 µl) were prepared as described previously (11) and contained $IF2_{mt}$ (26 nM), 12.5 µg poly(A,U,G), [^{35}S]fMet-tRNA (50 nM), 55S ribosomes (40 nM) and $IF3_{mt}$ or its derivatives (60 nM). Mixtures contained either 0.25 mM GTP or 0.5 mM GDPNP and were incubated for 10 min at 37°C. The amount of [^{35}S]fMet-tRNA bound to ribosomes was measured using a nitrocellulose filter-binding assay (3).

Binding of $IF3_{mt}$, $IF3_{mt}-\Delta N$ and $IF3_{mt}-\Delta NC$ to 28S subunits using surface plasmon resonance

The rate constants for the interaction of $IF3_{mt}$ with 28S subunits were determined using a Biacore 2000 biosensor instrument located in the UNC Macromolecular Interactions Facility. The rates of association and dissociation were measured by recording the change in refractive index

with time. The Running Buffer composition was 20 mM HEPES–KOH, pH 7.6, 7.5 mM $MgCl_2$, 100 mM KCl, 1 mM DTT, 0.5% glycerol and 0.01% surfactant P20 at a flow rate of 20 µl/min. CM5 chips (research grade) were activated by injecting 60 µl of 1:1 mixture of *N*-ethyl-*N*-(3-dimethylaminopropyl)carbodiimide hydrochloride (EDC) and *N*-hydroxysuccinimide (NHS) at a flow rate of 10 µl/min using the standard amine-coupling protocol (BIAapplication Handbook, Biacore). Following CM5 surface activation, 60 µl $IF3_{mt}$ (5 µg/ml) diluted in 5 mM sodium acetate, pH 4.5 was injected at a flow rate of 10 µl/min. Subsequently, 60 µl ethanolamine–hydrochloride was injected to deactivate any unreacted groups remaining. The extent of immobilization was ~200–400 RU on the surface including a control surface with avidin. A ~2000 RU surface was also prepared to examine the effect of high protein concentrations on the association and dissociation rates. The apparent rate of dissociation of 28S subunits from $IF3_{mt}$ on the surface depends on the concentration of coupled $IF3_{mt}$. The 2000 RU surface showed a 10-fold greater RU change after 28S injection than the 200 RU surface. However, abnormal dissociation rates were observed from these high density surfaces due to the rebinding of 28S subunits during the dissociation phase. Therefore, the surface with the lower level of immobilized $IF3_{mt}$ was used to study the interaction of $IF3_{mt}$ with 28S subunits. Small subunits were diluted in 200 µl Running Buffer to obtain a concentration either 25 or 75 nM and 60 µl of each solution was injected at a flow rate 20 µl/min. The RU change due to the binding of 28S subunits was obtained by subtracting the RU of the control surface (avidin bound at 200 RU) from the RU obtained from the surface containing $IF3_{mt}$. Surfaces were regenerated by injecting 10 µl of 20 mM HEPES–KOH, pH 7.6, 1 M KCl, 10 mM EDTA and 0.1% surfactant P20. The surface activity was tested after regeneration to verify that $IF3_{mt}$ remained active.

The association and dissociation rate constants were also verified by cysteine coupling. For cysteine coupling, the Running Buffer above was used except that no DTT was present. For thiol-coupling, the surface was activated with EDC/NHS and reactive disulfides were introduced with 80 mM PDEA in borate buffer at pH 8.5. $IF3_{mt}$ was coupled to the surface by disulfide exchange. The unreacted disulfides were deactivated by injecting 60 µl of a solution containing 50 mM cysteine and 1 M NaCl in 100 mM sodium acetate, pH 4.5 at a flow rate of 10 µl/min.

Calculation of the association and dissociation rate constants and the detailed analysis of surface plasma resonance (SPR) data was based on the approach described previously (35) and is described in detail in Supplementary Data.

RESULTS

Estimation of the K_d for the binding of $IF3_{mt}$ to 28S subunits and the role of the N- and C-terminal extensions on this binding using Microcon centrifugation

$IF3_{mt}$ contains N- and C-domains joined by a linker. Unlike the bacterial N- and C-domains, $IF3_{mt}$ contains

Table 1. The apparent equilibrium dissociation constant (K_d) for the binding of IF3$_{mt}$ and its extension truncated derivatives to 28S subunits using Microcon centrifugation and to 39S subunits using sucrose density gradient centrifugation

Protein	K_d for 28S (nM) (± 4 nM)	K_d for 39S[a] (nM)
IF3$_{mt}$	29	1500
IF3$_{mt}$−ΔN	26	250
IF3$_{mt}$−ΔC	29	170
IF3$_{mt}$−ΔNC	28	120

[a]The estimated K_d for the interactions of 39S subunits to IF3$_{mt}$ is estimated to be within 10–15%.

extensions of just over 30 residues at both the N- and C-termini (Figure 1). The structures of these extensions are not known. A model of IF3$_{mt}$ based on the structure of the N- and C-domains of *Bacillus stearothermophilus* IF3 (PDB coordinates 1 TIG) suggests that the N- and C-extensions will project towards the linker region (10). Previous data indicate that neither the N-terminal nor the C-terminal extension is required for the activity of IF3$_{mt}$ in promoting initiation complex formation on mitochondrial ribosomes (10). However, the C-terminal extension is important for the ability of IF3$_{mt}$ to facilitate the dissociation of fMet-tRNA bound to 28S subunits in the absence of mRNA.

The binding of IF3$_{mt}$ and its truncated derivatives to 28S subunits was measured using Microcon-100 centrifugation followed by colorimetric quantitation using antibodies against IF3$_{mt}$. The Microcon-100 has been used previously to study the binding of the *E. coli* ribosome recycling factor and IF3 to ribosomes (13,36). In the absence of 28S subunits, more than 90% of the IF3$_{mt}$ passed through the Microcon filter allowing the use of this method to measure the binding of IF3$_{mt}$ to 28S subunits using a calibration curve generated with known amounts of IF3$_{mt}$ (Supplementary Data, Figure S1A).

For determination of the apparent equilibrium dissociation constant, different concentrations of IF3$_{mt}$ or its derivatives were incubated with a fixed amount of 28S subunits, and the amount of IF3$_{mt}$ bound to 28S (28S–IF3$_{mt}$) was determined (Supplementary Data, Figure S1B). IF3$_{mt}$ binds to mitochondrial 28S subunits with a K_d of ~30 nM (Table 1). This value is similar to that reported for the binding of *E. coli* IF3 to 30S subunits (30–100 nM) (23,28,29,37,38). Deletion of the extensions had no effect on the apparent binding constant (Table 1) indicating that the major determinants for ribosomal subunit binding by IF3$_{mt}$ lie within the region homologous to the bacterial factors.

The K_d values for the interaction between IF3$_{mt}$ and 28S subunits did not change sharply with increasing KCl concentrations (29 nM at 40 mM KCl and 35 nM at 100 mM KCl). The association constant for *E. coli* IF3 binding to 30S subunits measured by fluorescence anisotropy decreased ~two-fold with increasing concentrations of NH$_4$Cl from 50 to 150 mM and decreased

2.5-fold with increasing Mg^{2+} concentration from 2.5 to 10 mM (39,40).

The results obtained from the Microcon centrifugation approach were verified using sucrose density gradient centrifugation. In this experiment, IF3$_{mt}$ was incubated with mitochondrial 28S subunits and applied to a 10–30% sucrose gradient. The IF3$_{mt}$ bound to the small subunits was separated from the free protein by centrifugation. The K_d value determined using the sucrose gradient centrifugation method was 35 nM, a value comparable to that obtained using the Microcon and confirming the validity of this approach.

Kinetics of the binding of IF3$_{mt}$ and its truncated derivatives to 28S subunits determined using surface plasma resonance

The rate constants for the association (k_{on}) and dissociation (k_{off}) of IF3$_{mt}$ from 28S subunits were determined by SPR. For these experiments, IF3$_{mt}$ was amine coupled to a Biacore CM5 chip. Avidin, which has an isoelectric point similar to that of IF3$_{mt}$ (pI = 10.5) was used on a control chip to check for non-specific binding of 28S subunits to basic proteins. IF3$_{mt}$, IF3$_{mt}$–ΔN and IF3$_{mt}$–ΔNC truncated derivatives were active after amine coupling and were capable of binding 28S subunits. However, the derivative that was truncated by removing the C-terminal extension alone was inactive when coupled to the surface.

The kinetics of the binding of IF3$_{mt}$ and its ΔNC truncated derivative at different concentrations of 28S subunits are shown in Figure 2. Conventionally, the rate constants in SPR measurements are determined using the built-in fitting equation provided in the Biacore software. However, we have opted to use the approach developed by O'Shannessy *et al.* (35) as described in Supplementary Data.

Three concentrations of 28S subunits were used for the determination of the rate constants, all of which gave similar dissociation rate constants. The rate constant for the dissociation of IF3$_{mt}$–ΔN from 28S subunits is very similar to that observed with full-length IF3$_{mt}$ (Table 2). However, IF3$_{mt}$–ΔNC shows about a 3.5-fold lower k_{off}, indicating that this derivative is released from the small subunit somewhat slower than the full-length factor. Association rate constants were determined from three data sets using Sigma Plot 2000 by global fitting (41). The association rate constant for the N-truncated derivative is slightly higher than full-length IF3$_{mt}$ (Table 2), while the rate of association of NC-truncated derivative is ~two-fold slower than that observed with IF3$_{mt}$. These results clearly indicate that the ΔNC-derivative of IF3$_{mt}$ not only dissociates more slowly from 28S subunits but also associates with the subunit more slowly relative to full-length IF3$_{mt}$.

Using the values obtained for k_{on} and k_{off}, the equilibrium dissociation constant (K_d) was calculated (Table 2). The values obtained are quite similar to those obtained by the Microcon and sucrose density gradient methods (Table 1). This observation indicates that there are no hidden intermediates in the interaction of IF3$_{mt}$ with 28S subunits. Once again, the equilibrium
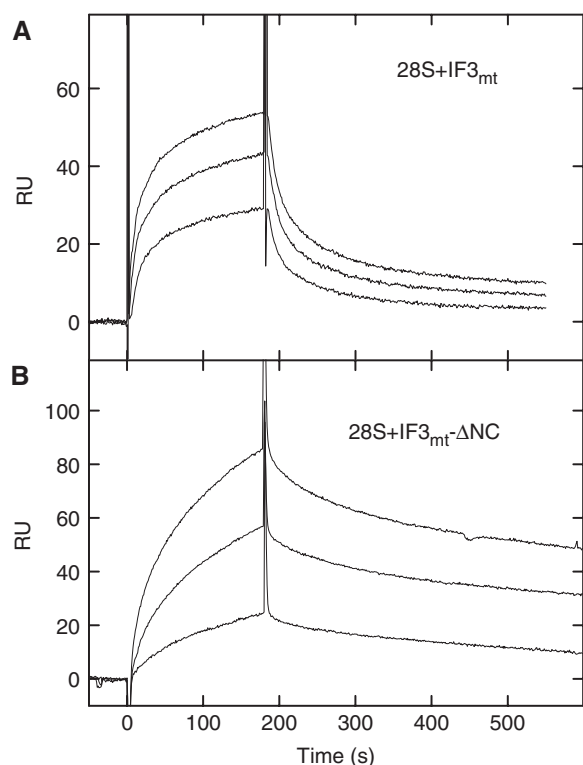
Figure 2. Association and dissociation rate constants for the binding of IF3$_{mt}$ to 28S subunits determined by surface plasmon resonance. (**A**) Sensorgram of IF3$_{mt}$ binding to 28S subunits. Ribosomes were diluted at different concentrations (25, 50 and 75 nM) and 60 μl of these dilutions were injected onto CM5 chips containing immobilized IF3$_{mt}$ or an avidin control at a flow rate of 20 μl/min. (**B**) Sensorgram of IF3$_{mt}$−ΔNC binding to 28S. In order to avoid crowding, the protein concentration was kept very low on the surface (the total RU change due to IF3$_{mt}$ coupling was ~200 to 400 RU). The RU values shown are due to the binding of 28S subunits to IF3$_{mt}$ (RU change due to IF3$_{mt}$−RU change due to avidin). Details of experimental conditions and procedures are given in Materials and Methods section.

Table 2. Kinetic constants (k_{on}, k_{off}) and calculated K_d values for the interaction of IF3$_{mt}$ and its truncated derivatives with the 28S subunit at 25°C

Protein	k_{on} (M^{-1} s^{-1})	k_{off} (s^{-1})	K_d (nM)
IF3$_{mt}$	$(3.80 \pm 0.15) \times 10^5$	$(1.35 \pm 0.02) \times 10^{-2}$	37 ± 9
IF3$_{mt}$−ΔN	$(5.18 \pm 0.14) \times 10^5$	$(1.21 \pm 0.02) \times 10^{-2}$	23 ± 5
IF3$_{mt}$−ΔNC	$(2.10 \pm 0.08) \times 10^5$	$(0.40 \pm 0.07) \times 10^{-2}$	20 ± 5

dissociation constants (K_d) for the truncated derivatives are not significantly different from that of IF3$_{mt}$. The reported K_d for the binding of *E. coli* IF3 to 30S subunits varies from 30 to 100 nM, although the values reported for k_{on} (10^4 to 10^8 M^{-1} s^{-1}) and k_{off} (0.44 to 20 s^{-1}) vary widely (28,29).

We verified the amine coupling results with thio-coupling of the factor to a Biacore chip. IF3$_{mt}$ has one cysteine residue in the C-domain which was used for the thio-coupling reaction. Interestingly, all of the truncated derivatives were better ligands for thio-coupling than
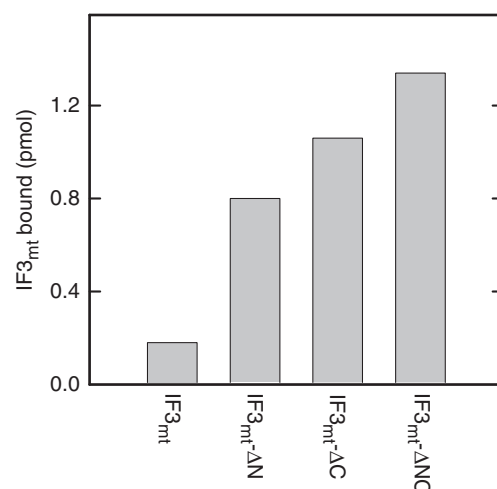

Figure 3. Effects of the N-terminal, C-terminal or both extensions on the binding of IF3$_{mt}$ to mitochondrial 39S subunits. Dot blot analysis of sucrose density gradient fractions was used to determine the amount of IF3$_{mt}$ or its deletion derivatives bound to 39S subunits as described in Materials and Methods section. Two controls were carried out, 39S subunits alone and IF3$_{mt}$ alone. These two control intensities were subtracted from 39S + IF3$_{mt}$ image intensities for the determination of bound protein to 39S subunits.

IF3$_{mt}$. However, the coupling of the derivatives to the surface was not stable and they were exchanged with cysteine during the surface deactivation step used to remove excess thio groups. Thus, we are not able to measure the rate of association and dissociation of 28S subunits on the thio-coupled truncated derivatives of IF3$_{mt}$. The association and dissociation rate constants for the interaction of full-length, thio-coupled, IF3$_{mt}$ with 28S subunits are 2.9×10^5 M^{-1} s^{-1} and 1.28×10^{-2} s^{-1}, respectively. These values are very similar to those obtained with amine coupling indicating that the amine coupling does not change the conformation of IF3$_{mt}$ or deactivate the protein.

Interaction of IF3$_{mt}$ and its deletion derivatives with the large mitochondrial ribosomal subunits (39S)

For the determination of binding constants, ribosomes or ribosomal subunits must be nearly pure. Samples of 39S subunits were purified through two successive sucrose density gradients. The amount of 28S contamination in these 39S preparations was estimated to be 2% based on an fMet-tRNA binding assay and ~6% using peak fits of the sucrose density gradient absorbance profile. In addition, there was a small amount of contamination with 55S monosomes. As a result of this level of cross-contamination, neither the Microcon nor the SPR method could be used for the determination of the binding constant of IF3$_{mt}$ to 39S subunits. The binding of IF3$_{mt}$ to 39S subunits was, therefore, examined by sucrose density gradient centrifugation followed by immunological detection (Supplementary Data, Figure S2). This analysis clearly indicates that IF3$_{mt}$ binds to 39S subunits to a small extent (Figure 3). The apparent K_d value for this interaction was estimated assuming that the 39S subunits

are 100% active and was calculated to be $1.5 \, \mu M$ (Table 1). This value is 50-fold weaker than the binding of $IF3_{mt}$ to 28S subunits indicating that, as expected, the main site of interaction between $IF3_{mt}$ and the ribosome is with the small subunit. Surprisingly, removal of the N-terminal extension, the C-terminal extension or both extensions enhanced the interaction of $IF3_{mt}$ with 39S subunits considerably (Figure 3). Indeed without the N- and C-terminal extensions $IF3_{mt}$ has only a four-fold greater affinity for 28S subunits than for 39S subunits. This observation suggests that the extensions on $IF3_{mt}$ may have evolved, in part, to reduce the affinity of this factor for 39S subunits.

Binding of $IF3_{mt}$ to 55S ribosomes

At low Mg^{2+} concentrations 55S ribosomes produce substantial amounts of 28S and 39S subunits, whereas at high Mg^{2+} concentrations most of the 55S ribosomes are present as monosomes. Due to the equilibrium between the 55S ribosome and its subunits, and the effect of $IF3_{mt}$ on this equilibrium, neither the Microcon assay nor SPR could be used to examine whether IF3 interacts with 55S particles. Hence, the interaction between 55S ribosomes and $IF3_{mt}$ was examined using sucrose density gradient centrifugation followed by immunological detection. Two Mg^{2+} concentrations (7.5 and 20 mM) were used. At $7.5 \, mM \, Mg^{2+}$, most of the $IF3_{mt}$ was bound to 28S subunits, and only small amounts of $IF3_{mt}$ were detected in 39S and 55S regions of the gradient (data not shown). At $20 \, mM \, Mg^{2+}$, the ribosomes were primarily present as 55S particles. No binding of $IF3_{mt}$ could be detected to the intact monosomes (data not shown). $IF3_{mt}-\Delta NC$ had weak interactions with 55S monosomes even with an apparent K_d value obtained of $1.3 \, \mu M$. The strong affinity of this derivative for 28S and 39S subunits apparently gives rise to a detectable interaction with tightly coupled 55S monosomes. *E. coli* IF3, which corresponds structurally to $IF3_{mt}-\Delta NC$ also binds weakly to 70S ribosomes ($K_d = 3 \, \mu M$) (42).

Dissociation of 55S ribosomes by $IF3_{mt}$ and its deletion derivatives

Bacterial IF3 has five different roles in initiation complex formation, one of which is to dissociate 70S ribosomes into 30S and 50S subunits, thus supplying 30S subunits for initiation complex formation (17). Previous observations (11) suggest that $IF3_{mt}$, like bacterial IF3, can promote the dissociation of ribosomes. To examine the role of the N- and C-terminal extensions on this activity, mitochondrial ribosomes were incubated with $IF3_{mt}$ or its deletion derivatives, and the distribution of ribosomal particles was examined by sucrose density gradient centrifugation (Figure 4). At the Mg^{2+} concentration used in these experiments (5 mM), most of the ribosomes are present as 55S particles in the absence of $IF3_{mt}$. As expected, incubation of the ribosomes with $IF3_{mt}$ leads to a significant shift in the equilibrium resulting in the accumulation of 28S and 39S subunits. Deletion of the N-terminal extension had only a minor effect on the ability of $IF3_{mt}$ to promote dissociation. However, removal of
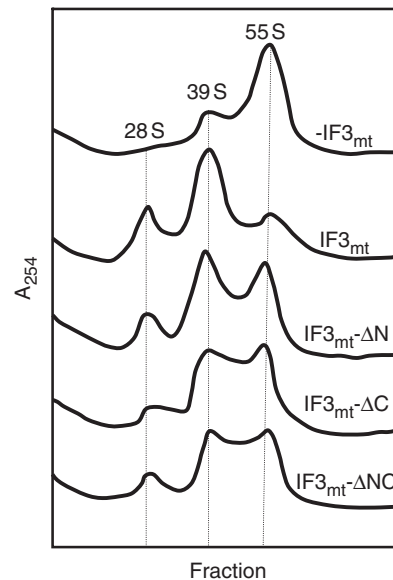

Figure 4. Effect of $IF3_{mt}$ and its truncated derivatives on the dissociation of mitochondrial ribosomes. Fractionation profiles of mitochondrial 55S ribosomes after centrifugation on a 10–30% sucrose gradient in 5 mM Mg^{2+}. Mitochondrial 55S ribosomes (56 nM) were incubated at 5 mM $MgCl_2$ in the absence and presence of $IF3_{mt}$ or its derivatives (350 nM) at 37°C for 15 min. The samples were then placed on ice for 10 min and subsequently layered on a 10–30% sucrose density gradient and analysed as described in Materials and Methods section.

the C-terminal extension ($IF3_{mt}-\Delta C$) or both the N- and C-terminal extensions ($IF3_{mt}-\Delta NC$) reduced the ability of $IF3_{mt}$ to promote subunit dissociation. Further, the gradient patterns obtained with these derivatives were broad and complex suggesting that the subunits had a tendency to partially reassociate during centrifugation when these derivatives were used. This result agrees with the idea that the C-terminal extension plays a role in preventing the interaction of $IF3_{mt}$ with the 39S subunit creating cleaner subunit dissociation patterns.

Role of extensions in fMet-tRNA binding to mitochondrial 55S ribosomes in the presence of GTP and GDPNP

The activities of the full-length $IF3_{mt}$ and its deletion derivatives in initiation complex formation on bovine 55S and *E. coli* 70S ribosomes have been described (10). In these experiments, the deletion derivatives were somewhat more active than full-length $IF3_{mt}$. The promotion of initiation complex formation could be due to an increase in 39S joining forming the more stable 55S initiation complex, which occurs more readily, particularly when the C-terminal extension is deleted. $IF3_{mt}$ also destabilizes the binding of fMet-tRNA to 28S subunits in the absence of mRNA. Deletion of the C-terminal extension removes this destabilizing effect and allows the detection of fMet-tRNA bound in the absence of mRNA which would be measured in this assay (10).

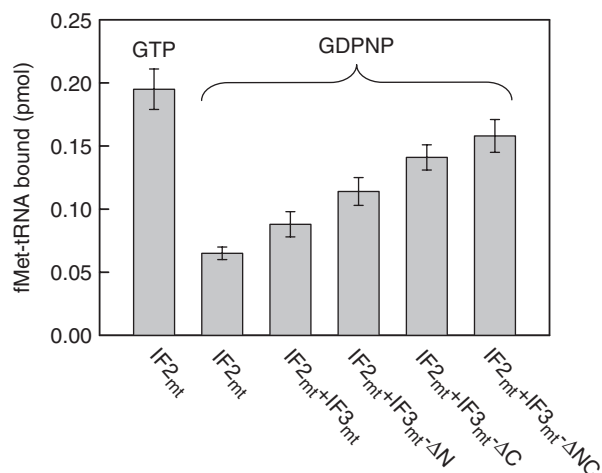When GDPNP was substituted for GTP in the fMet-tRNA binding assay (Figure 5), significantly less binding

Figure 5. Effect of IF3 and derivatives on initiation complex formation with GDPNP. [^{35}S]fMet-tRNA binding to mitochondrial 55S particles (40 nM) was tested in the presence of saturating amount of IF3$_{mt}$, IF3$_{mt}$−ΔN, IF3$_{mt}$−ΔC and IF3$_{mt}$−ΔNC (60 nM) and 26 nM IF2$_{mt}$ in the presence of 0.5 mM GDPNP or 0.25 mM GTP as indicated. A blank representing the amount of label retained on the filter in the absence of IF2$_{mt}$ has been subtracted from samples that did not contain IF3$_{mt}$ (0.016 pmol) and that contained IF3$_{mt}$ (0.023 pmol).

was observed in the presence of IF2$_{mt}$ as expected. This difference reflects the inability of IF2$_{mt}$ to recycle when GDPNP is used. IF3$_{mt}$ had no significant effect on fMet-tRNA binding to 55S particles in the presence of GDPNP since the amount of IF2$_{mt}$ used in this experiment was limited and IF2$_{mt}$ remained trapped on ribosomes in the presence of GDPNP. However, when the N- and C-terminal extensions were deleted (IF3$_{mt}$−ΔNC) the amount of fMet-tRNA bound in the presence of GDPNP was enhanced and approached the value obtained in the presence of GTP (Figure 5). Both the N- and C-terminal extensions appeared to have a partial effect in this process. This observation suggests that deletion of the extensions in IF3$_{mt}$ facilitates the formation of the 55S complex and may reduce the affinity of IF2$_{mt}$ for the ribosome or for the small subunit allowing this factor to recycle even in the presence of GDPNP.

DISCUSSION

In the present study, we have examined the interaction of IF3$_{mt}$ with mitochondrial ribosomes and have investigated the roles of the N- and C-terminal extensions on these interactions. The extensions observed in human IF3$_{mt}$ are reminiscent of the large extensions present in *Euglena gracilis* chloroplast IF3 (IF3$_{chl}$), which has an N-terminal extension of over 100 residues and a C-terminal extension of just over 60 residues. The extensions in IF3$_{chl}$ reduce the binding of this factor to chloroplast 30S ribosomal subunits ~100-fold and inhibit its activity in initiation complex formation *in vitro* (43–45). *Myxococcus xanthus* IF3 has a C-terminal extension of over 60 amino acids (46,47). This extension is important for vegetative and

developmental functions in this organism but is not required for cell viability.

Removal of the N- and C-terminal extensions in human IF3$_{mt}$ slightly promotes initiation complex formation on 55S ribosomes. The first difference between the full-length IF3$_{mt}$ and its truncated derivatives was the observation that the C-truncated derivative cannot dissociate fMet-tRNA bound to 28S subunits in the absence of mRNA (10). This observation suggests that there may be a role for this region of IF3$_{mt}$ in the destabilization of incorrect initiation complexes. In the current work, we have shown that, unlike the extensions in *E. gracilis* IF3$_{chl}$, the extensions on IF3$_{mt}$ do not affect the binding of this factor to the small ribosomal subunit. However, the extensions appear to play a major role in preventing this factor from binding to the large ribosomal subunit. Full-length IF3$_{mt}$ has a very weak interaction with 39S subunits. Deletion of either the N- or C-terminal extension leads to a factor with a significantly higher affinity for the large subunit. The extensions appear to work together in reducing affinity for the 39S subunit. Further, deletion of the extensions results in the formation of a 55S initiation complex in which IF2$_{mt}$ appears to be more readily released.

These observations lead us to propose a model (Figure 6) in which a 28S initiation complex, including IF2$_{mt}$, IF3$_{mt}$, fMet-tRNA and mRNA is first formed. Upon binding of the 39S subunit, IF3$_{mt}$ is normally released and a stable 55S initiation complex forms. In the presence of GDPNP, IF2$_{mt}$ is not released and IF2$_{mt}$ does not recycle. However, when the N- and C-terminal extensions of IF3$_{mt}$ are removed, the remaining region of IF3$_{mt}$ has a significant affinity for 39S subunits. Under these conditions, the large subunit joins the 28S subunits readily but is probably not correctly positioned. Under these conditions, the binding of IF2$_{mt}$ is destabilized leading to the release of this factor even in the presence of GDPNP. Thus, one role for the extensions that have evolved at the termini of IF3$_{mt}$ is to reduce the affinity of this factor for the protein-rich 39S subunit preventing improper joining of the large and small ribosomal subunits during initiation complex formation.

SUPPLEMENTARY DATA

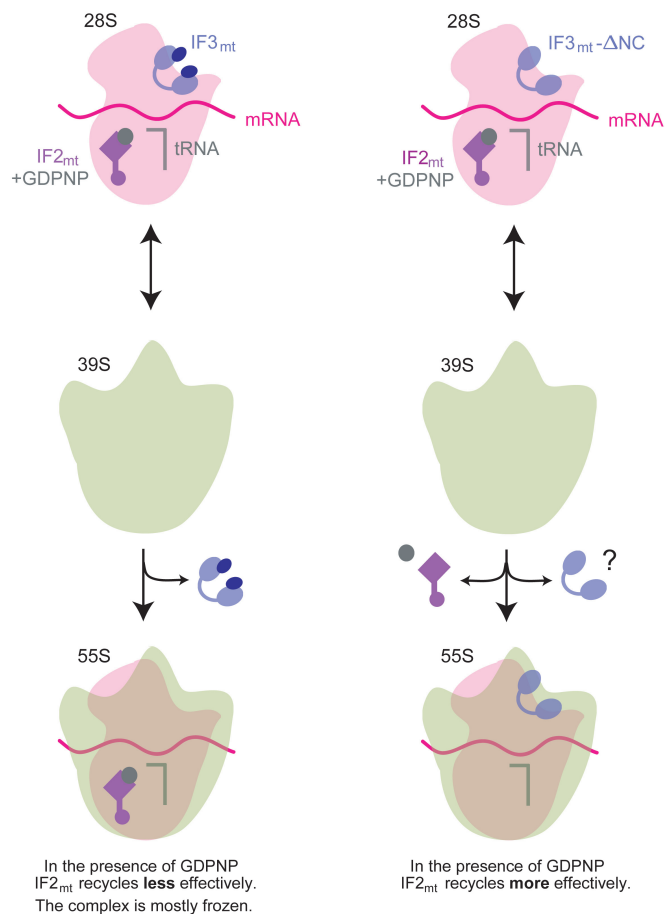Supplementary Data are available at NAR Online.

ACKNOWLEDGEMENTS

Figure 6. Model for the proposed role of the extensions of IF3$_{mt}$ in initiation complex formation. IF3$_{mt}$ binding and dissociation is shown in the left panel and IF3$_{mt}$−ΔNC in the right panel. IF3$_{mt}$ and IF3$_{mt}$−ΔNC dissociate 55S ribosomes and bind to 28S subunits. IF3$_{mt}$ has very weak interactions with 39S subunits and is released rapidly upon 39S subunits joining. In the presence of GDPNP, IF2$_{mt}$ is then frozen on the ribosome and cannot recycle properly. IF3$_{mt}$−ΔNC has a strong affinity for 39S subunits and its rate of dissociation from ribosomes is slow when 39S subunits join. Therefore, IF3$_{mt}$−ΔNC does not permit the proper joining of the 39S subunit. Under these conditions, IF2$_{mt}$ binding is destabilized and is released from the initiation complex even in the presence of GDPNP.

REFERENCES

1. O'Brien,T.W., Denslow,N.D., Faunce,W., Anders,J., Liu,J. and O'Brien,B. (1993) Structure and function of mammalian mitochondrial ribosomes. In Nierhaus,K., Franceschi,F., Subramanian,A., Erdmann,V. and Wittmann-Liebold,B. (eds), *The Translational Apparatus: Structure, Function Regulation and Evolution*. Plenum Press, New York, pp. 575–586.
2. Sharma,M.R., Koc,E.C., Datta,P.P., Booth,T.M., Spremulli,L.L. and Agrawal,R.K. (2003) Structure of the mammalian mitochondrial ribosome reveals an expanded functional role for its component proteins. *Cell*, **115**, 97–108.
3. Liao,H.-X. and Spremulli,L.L. (1991) Initiation of protein synthesis in animal mitochondria: purification and characterization of translational initiation factor 2. *J. Biol. Chem.*, **266**, 20714–20719.
4. Liao,H.-X. and Spremulli,L.L. (1990) Identification and initial characterization of translational initiation factor 2 from bovine mitochondria. *J. Biol. Chem.*, **265**, 13618–13622.
5. Spencer,A.C. and Spremulli,L.L. (2004) Interaction of mitochondrial initiation factor 2 with mitochondrial (f)Met-tRNA. *Nucleic Acids Res.*, **32**, 5464–5470.
6. Spencer,A.C. and Spremulli,L.L. (2005) The interaction of mitochondrial translational initiation factor 2 with the small ribosomal subunit. *Biochim. Biophys. Acta—Proteins Proteomics*, **1750**, 69–81.
7. Ma,J., Farwell,M., Burkhart,W. and Spremulli,L.L. (1995) Cloning and sequence analysis of the cDNA for bovine mitochondrial translational initiation factor 2. *Biochim. Biophys. Acta*, **1261**, 321–324.
8. Ma,J. and Spremulli,L.L. (1996) Expression, purification and mechanistic studies of bovine mitochondrial translational initiation factor 2. *J. Biol. Chem.*, **271**, 5805–5811.
9. Ma,L. and Spremulli,L.L. (1995) Cloning and sequence analysis of the human mitochondrial translational initiation factor 2 cDNA. *J. Biol. Chem.*, **270**, 1859–1865.
10. Bhargava,K. and Spremulli,L.L. (2005) Role of the N- and C-terminal extensions on the activity of mammalian mitochondrial translational initiation factor 3. *Nucleic Acids Res.*, **33**, 7011–7018.
11. Koc,E.C. and Spremulli,L.L. (2002) Identification of mammalian mitochondrial translational initiation factor 3 and examination of its role in initiation complex formation with natural mRNAs. *J. Biol. Chem.*, **277**, 35541–35549.
12. Dottavio-Martin,D., Suttle,D.P. and Ravel,J.M. (1979) The effects of initiation factors IF-1 and IF-3 on the dissociation of Escherichia coli 70 S ribosomes. *FEBS Lett.*, **97**, 105–110.
13. Dallas,A. and Noller,H.F. (2001) Interaction of translation initiation factor 3 with the 30S ribosomal subunit. *Mol. Cell*, **8**, 855–864.
14. Paci,M., Pon,C., Lammi,M. and Gualerzi,C. (1984) Structure-function relationship in *Escherichia coli* translational initiation factors. Characterization of IF-3 by high resolution ^{1}H NMR spectroscopy. *J. Biol. Chem.*, **259**, 9628–9634.
15. La Teana,A., Gualerzi,C. and Brimacombe,R. (1995) From stand-by to decoding site. Adjustment of the mRNA on the 30 S subunit under the influence of the initiation factors. *RNA*, **1**, 772–782.
16. Antoun,A., Pavlov,M.Y., Lovmar,M. and Ehrenberg,M. (2006) How initiation factors tune the rate of initiation of protein synthesis in bacteria. *EMBO J.*, **25**, 2539–2550.
17. Petrelli,D., LaTeana,A., Garofalo,C., Spurio,R., Pon,C.L. and Gualerzi,C.O. (2001) Translation initiation factor IF3: two domains, five functions, one mechanism? *EMBO J.*, **20**, 4560–4569.
18. McCutcheon,J., Agrawal,R., Philips,S.M., Grassucci,R., Gerchman,S., Clemons,W.M., Ramakrishnan,V. and Frank,J. (1999) Location of translational initiation factor IF3 on the small ribosomal subunit. *Proc. Natl Acad. Sci. USA*, **96**, 4301–4306.
19. Fabbretti,A., Pon,C.L., Hennelly,S.P., Hill,W., Lodmell,J. and Gualerzi,C. (2007) The real-time path of translation factor IF3 onto and off the ribosome. *Mol. Cell*, **25**, 285–296.
20. Laursen,B.S., Sorensen,H.P., Mortensen,K.K. and Sperling-Petersen,H.U. (2005) Initiation of protein synthesis in bacteria. *Microbiol. Mol. Biol. Rev.*, **69**, 101–123.
21. Antoun,A., Pavlov,M.Y., Lovmar,M. and Ehrenberg,M. (2006) How initiation factors maximize the accuracy of tRNA selection in initiation of bacterial protein synthesis. *Mol. Cell*, **23**, 183–193.
22. Weiel,J., Hershey,J. and Levison,S. (1978) Fluorescence polarization studies of the binding of fluorescein-labeled initiation factor IF3 to 30 S ribosomal subunits from *Escherichia coli*. *FEBS Lett.*, **87**, 103–106.
23. Tapprich,W., Goss,D. and Dahlberg,A. (1989) Mutation at position 91 in *Escherichia coli* 16 S ribosomal RNA affects processes involved in the initiation of protein synthesis. *Proc. Natl Acad. Sci. USA*, **86**, 4927–4931.
24. Box,R., Woolley,P. and Pon,C. (1981) The binding of dansylated initiation factor 3 to the 30-S subunit of *Escherichia coli*: a fluorimetric and biochemical study. *Eur. J. Biochem.*, **116**, 93–99.
25. Pioletti,M., Schlunzen,F., Harms,J., Zarivach,R., Gluhmann,M., Avila,H., Bashan,A., Bartels,H., Auerbach,T. *et al.* (2001) Crystal structures of complexes of the small ribosomal subunit with tetracycline, edeine and IF3. *EMBO J.*, **20**, 1829–1839.
26. Moazed,D., Samaha,R.R., Gualerzi,C. and Noller,H.F. (1995) Specific protection of 16 S rRNA by translational initiation factors. *J. Mol. Biol.*, **248**, 207–210.
27. Ehresmann,C., Moine,H., Mougel,M., Dondon,J., Grunberg-Manago,M., Ebel,J.P. and Ehresmann,B. (1986)

Cross-linking of initiation factor IF3 to *Escherichia coli* 30S ribosomal subunit by trans-diamminedichloroplatinum(II): characterization of two cross-linking sites in 16S rRNA; a possible way of functioning for IF3. *Nucleic Acids Res.*, **14**, 4803–4821.

28. Woolley,P. and Box,R. (1979) The rate of binding of initiation factor 3 to the 30 S ribosomal subunit of *Escherichia coli*. *FEBS Lett.*, **108**, 433–435.

29. Goss,D.J., Parkhurst,L.J. and Wahba,A.J. (1982) Kinetic studies on the interaction of chain initiation factor 3 with 70 S *Escherichia coli* ribosomes and subunits. *J. Biol. Chem.*, **257**, 10119–10127.

30. Schmitt,E., Guillon,J.M., Meinnel,T., Mechulam,Y., Dardel,F. and Blanquet,S. (1996) Molecular recognition governing the initiation of translation in *Escherichia coli*. A review. *Biochimie*, **78**, 543–554.

31. Biou,V., Shu,F. and Ramakrishnan,V. (1995) X-ray crystallography shows that translational initiation factor IF3 consists of two compact a/b domains linked by an a-helix. *EMBO J.*, **14**, 4056–4064.

32. Matthews,D.E., Hessler,R.A., Denslow,N.D., Edwards,J.S. and O'Brien,T.W. (1982) Protein composition of the bovine mitochondrial ribosome. *J. Biol. Chem.*, **257**, 8788–8794.

33. Graves,M. and Spremulli,L.L. (1983) Activity of *Euglena gracilis* chloroplast ribosomes with prokaryotic and eukaryotic initiation factors. *Arch. Biochem. Biophys.*, **222**, 192–199.

34. Grasso,D.G., Christian,B.E., Spencer,A.C. and Spremulli,L.L. (2007) Overexpression and purification of mitochondrial transla-tional initiation factor 2 and initiation factor 3. In Lorsch,J. (ed), *Translation Initiation: Reconstituted Systems and Biophysical Methods*, Vol. 430, (Methods in Enzymology). Academic Press, New York, pp. 59–78.

35. O'Shannessy,D.J., Brigham-Burke,M., Soneson,K.K., Hensley,P. and Brooks,I. (1993) Determination of rate and equilibrium binding constants for macromolecular interactions using surface plasmon resonance: use of nonlinear least squares analysis methods. *Anal. Biochem.*, **212**, 457–468.

36. Hirokawa,G., Kiel,M.C., Muto,A., Kawai,G., Igarashi,K., Kaji,H. and Kaji,A. (2002) Binding of ribosome recycling factor to ribosomes, comparison with tRNA. *J. Biol. Chem.*, **277**, 35847–35852.

37. Weiel,J. and Hershey,J.W. (1982) The binding of fluorescein-labeled protein synthesis initiation factor 2 to *Escherichia coli* 30 S ribosomal subunits determined by fluorescence polarization. *J. Biol. Chem.*, **257**, 1215–1220.

38. Subramanian,A.R. and Davis,B.D. (1970) Activity of initiation factor F3 in dissociating *Escherichia coli* ribosomes. *Nature*, **228**, 1273–1275.

39. Weiel,J. and Hershey,J.W. (1981) Fluorescence polarization studies of the interaction of *Escherichia coli* protein synthesis initiation factor 3 with 30S ribosomal subunits. *Biochemistry*, **20**, 5859–5865.

40. Pon,C.L. and Gualerzi,C. (1976) The role of 16S rRNA in ribosomal binding of IF-3. *Biochemistry*, **15**, 804–811.

41. Haque,M.E., Koppaka,V., Axelsen,P.H. and Lentz,B.R. (2005) Properties and structures of the influenza and HIV fusion peptides on lipid membranes: implications for a role in fusion. *Biophys. J.*, **89**, 3183–3194.

42. Firpo,M., Connelly,M., Goss,D. and Dahlberg,A. (1996) Mutations at two invariant nucleotides in the 3′-minor domain of *Escherichia coli* 16 S rRNA affecting translational initiation and initiation factor 3 function. *J. Biol. Chem.*, **271**, 4693–4698.

43. Yu,N.-J. and Spremulli,L.L. (1997) Structural and mechanistic studies on chloroplast translational initiation factor 3 from *Euglena gracilis*. *Biochemistry*, **36**, 14827–14835.

44. Yu,N.-J. and Spremulli,L.L. (1998) Regulation of the activity of chloroplast translational initiation factor 3 by NH_2- and COOH-terminal extensions. *J. Biol. Chem.*, **273**, 3871–3877.

45. Lin,Q., Yu,N.-J. and Spremulli,L.L. (1996) Expression and functional analysis of *Euglena gracilis* chloroplast initiation factor 3. *Plant Mol. Biol.*, **32**, 937–945.

46. Cheng,Y., Kalman,L. and Kaiser,D. (1994) The dsg gene of *Myxococcus xanthus* encodes a protein similar to translation initiation factor IF3. *J. Bacteriol.*, **176**, 1427–1433.

47. Kalman,L., Cheng,Y. and Kaiser,D. (1994) The *Myxococcus xanthus* dsg gene product performs functions of translation initiation factor 3 in vivo. *J. Bacteriol.*, **176**, 1434–1442.